Ferromagnetic Resonance Investigations of Cobalt Implanted Polyimides

Rameev, B.Z.; Okay, C.; Yildiz, F.; Khaibullin, R.I.; Popok, Vladimir; Aktas, B.

Published in:
Journal of Magnetism and Magnetic Materials

Publication date:
2004

Document Version
Publisher's PDF, also known as Version of record

Available online at www.sciencedirect.com
SCIENCE DIRECT®
ELSEVIER
Journal of Magnetism and Magnetic Materials 278 (2004) 164–171
Journal of magnetism and magnetic materials
www.elsevier.com/locate/jmmm

Ferromagnetic resonance investigations of cobalt-implanted polyimides

B. Rameev[a,b,*], C. Okay[c], F. Yildiz[a], R.I. Khaibullin[a,b], V.N. Popok[d], B. Aktas[a]

[a] Department of Physics, Gebze Institute of Technology, Istanbul C. 101, P.B. 141, 41400 Gebze- Kocaeli, Turkey
[b] Kazan Physical-Technical Institute, 10/7, Sibirsky Trakt, 420029 Kazan, Russia
[c] Marmara University, 81040 Goztepe-Istanbul, Turkey
[d] Gothenburg University and Chalmers University of Technology, 41296 Gothenburg, Sweden

Received 16 October 2003; received in revised form 3 December 2003

Abstract

Co^+ ions of 40 keV were implanted in thin polyimide foils with doses in the range of $(0.25–1.50) \times 10^{17}$ ions/cm^2 at ion current densities of 4, 8 and 12 μA/cm^2. The cobalt-implanted polymer foils were annealed at a temperature of 300°C for 2 h in vacuum. Both the as-implanted and post-annealed samples were investigated by the ferromagnetic resonance (FMR) technique supplemented by transmission electron microscopy (TEM). TEM investigations showed that the implantation results in the formation of cobalt granules in the irradiated polymer layer with the thickness of about 70 nm. The mean lateral size of cobalt granules varied within 5–20 nm depending on the dose. The annealing of the implanted samples induced coalescence of the cobalt granules and increase of their lateral sizes. No FMR signals were found for the as-prepared polymer foils implanted by cobalt ions at low current density of 4 μA/cm^2. FMR signals were observed for the as-prepared samples implanted at higher ion current densities of 8 and 12 μA/cm^2 as well as for all annealed samples. The values of the effective magnetisation were extracted from the FMR spectra measured at different sample orientations in the applied magnetic field. Dose dependencies of the FMR absorption intensity and effective magnetisation were obtained for the annealed films. The magnetic properties of the synthesised cobalt–polymer composite materials and their modification due to the annealing treatment are discussed.

PACS: 75.50.Tt; 75.70.−i; 76.30.Fc; 76.50.+g

Keywords: Ion implantation; Granular magnetic films; Ferromagnetic resonance

1. Introduction

Magnetic properties of nanoparticles embedded in a dielectric host is a topic of extensive investigations due to the wide range of potential applications for such materials including magnetic recording, magnetosensor electronics, magnetooptical devices, etc. (see, for example, Ref. [1]). There is a number of different techniques to prepare nanoparticles dispersed in various dielectric matrixes and ion implantation is a widely used method. This technique, which has routinely being applied in the production of planar semiconductor

*Corresponding author. Department of Physics, Gebze Institute of Technology, Istanbul C. 101, P.B. 141, 41400 Gebze- Kocaeli, Turkey. Tel.: +90-262-6538497; fax: +90-262-6538490.
E-mail address: rameev@gyte.edu.tr (B. Rameev).

0304-8853/$ - see front matter © 2003 Elsevier B.V. All rights reserved.
doi:10.1016/j.jmmm.2003.12.332

devices, has an advantage for magnetoelectronic applications due to its easy integration in the traditional technological process.

Precipitation phenomena in different dielectrics (alumina, silica, glasses, etc.) implanted by high doses ($>10^{16}$ ions/cm^2) of transition metal ions have been studied extensively in the last two decades [2–4, and references therein]. For example, nanocrystalline cobalt particles are characterised by high saturation magnetisation and coercive force and have a potential to be used in high-density recording media [5] and magnetic sensors based on the giant tunnel-type magnetoresistance effect [6]. Meanwhile, polymer materials are widely used in various technological applications because of their unique properties such as low density, plasticity and ability to form intricate shapes, versatile electrical and optical properties and low manufacturing cost. However, the synthesis of magnetic metal phases with required parameters by ion implantation in polymers is still under development [7–11]. Therefore, it is a subject of great interest to apply the ion implantation technique for synthesis of nanoparticles in various polymers and to study the magnetic properties of such nanocomposites.

In the present study, composite material was formed by the high dose implantation of cobalt ions in polyimide (PI) foils. The formation of nanoscale cobalt particles in thin irradiated layers of the polymer was detected by transmission electron microcopy (TEM). The ferromagnetic resonance (FMR) technique has been used to investigate the magnetic properties of the cobalt–PI nanogranular films.

2. Experimental

PI foils 40 μm in thickness were implanted with 40 keV Co^+ ions to dose range of $(0.25–1.50)\times 10^{17}$ ions/cm^2 at an ion current density of 4 μA/cm^2. Two more samples were also prepared by implantation with the dose of 1.25×10^{17} ions/cm^2 at the ion current densities of 8 and 12 μA/cm^2. The sample holder was water cooled during the irradiation to prevent sample overheating and thermal degradation. The implanted PI foils were annealed at a temperature of 300°C for 2 h in vacuum of $\sim 10^{-6}$ Torr. The microstructure of both the as-implanted and subsequently annealed samples was studied by TEM using a TESLA-BS500 microscope. The specimens for on-plane TEM studies were prepared by chemical etching of the non-irradiated part of the PI foils, as described elsewhere [12].

FMR absorption spectra of the cobalt-implanted PI foils were obtained on a Bruker EMX Electron Spin Resonance (ESR) spectrometer at X-band frequency of 9.5 GHz. The FMR spectra were recorded at room temperature and for various orientations of the implanted surface with respect to the applied DC magnetic field (H). As usual, the field derivative of the microwave power absorption (dP/dH) was recorded as a function of the DC field. The resonance field (H_r) was defined as the value of the applied magnetic field, at which the dP/dH curve intersects a baseline. To obtain an intensity of ESR signal the double digital integration of the ESR curves was performed by using the *Bruker WINEPR* software package. To compare arbitrary intensities of the FMR signals, the values received by the integration were normalised per unit area of the samples.

3. Results and discussion

3.1. TEM of cobalt-implanted PIs

According to the TEM cross-sectional and Rutherford back-scattering studies presented in Ref. [13], the synthesised cobalt granular layer is located at depths ranging from 30 to 100 nm under the PI surface. TEM plane images of the near-surface region of the PI foils implanted with a dose of 1.25×10^{17} ions/cm^2 at the ion current density of 4 μA/cm^2 (A) and subsequently annealed (B) are presented in Fig. 1. The lateral size of the largest particles in the as-implanted PI is estimated to be smaller than 20 nm and a rather broad particle size distribution with a large fraction of very small granules may be anticipated for this sample. The lateral sizes of granules observed in the annealed sample (Fig. 1B) are in the range of 5–20 nm. The figure also indicates that the annealing procedure

induces the particle coagulation and coalescence, increasing the lateral size of the granules. The area density of the granules estimated from this image is about $10^{10}\,cm^{-2}$.

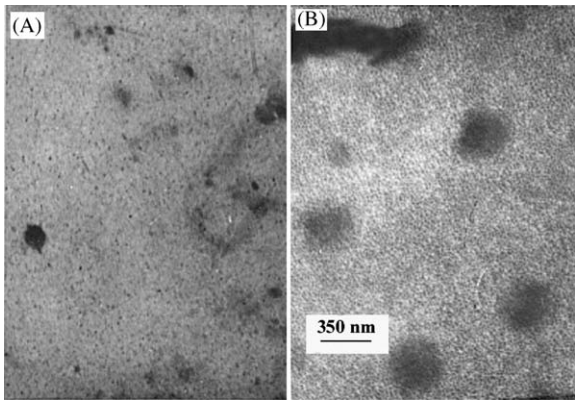

Fig. 1. TEM plane images of PI foils implanted with dose of 1.25×10^{17} ions/cm^2 at ion current density of $4\,\mu A/cm^2$: (A) as-implanted sample; (B) annealed sample. The large black spots are not related to the cobalt granules but appear from polymer remainders as a result of etching procedure.

3.2. FMR study of cobalt-implanted PIs

No ESR signals are observed for the as-prepared samples implanted in the dose range of $(0.25–1.50)\times10^{17}$ ions/cm^2 at the ion current density of $4\,\mu A/cm^2$. The resonance signal is only observed for films implanted at higher current densities of 8 and $12\,\mu A/cm^2$. An intense signal is also observed for all annealed samples (Fig. 2) except for the lowest dose of 0.25×10^{17} ions/cm^2. The signal is found to be slightly dependent on the film orientation in the magnetic field for low implantation dose but shows a strong angular dependence for high doses. This signal dependence on the sample orientation is similar to that found for the FMR in thin magnetic films. For the static magnetic field parallel to the film plane ($\theta_H = 90°$) the FMR signal is shifted to the low-field region, for the field perpendicular to the plane ($\theta_H = 0°$) the signal is shifted to the high-field values. Fig. 3 shows the FMR spectra for PI implanted with a fixed dose of 1.25×10^{17} ions/cm^2 at the different ion current densities and subsequently annealed. Angular dependencies of the resonance field (H_r)

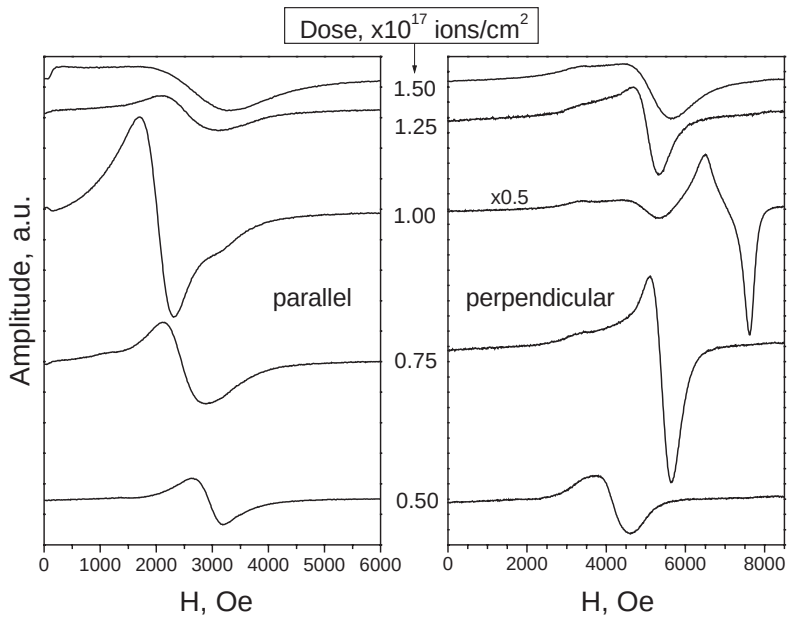

Fig. 2. FMR spectra of the samples implanted with different doses and subsequently annealed in vacuum. The spectra, measured at parallel and perpendicular orientation of film plane to the magnetic field, are presented at left and right panels, respectively.

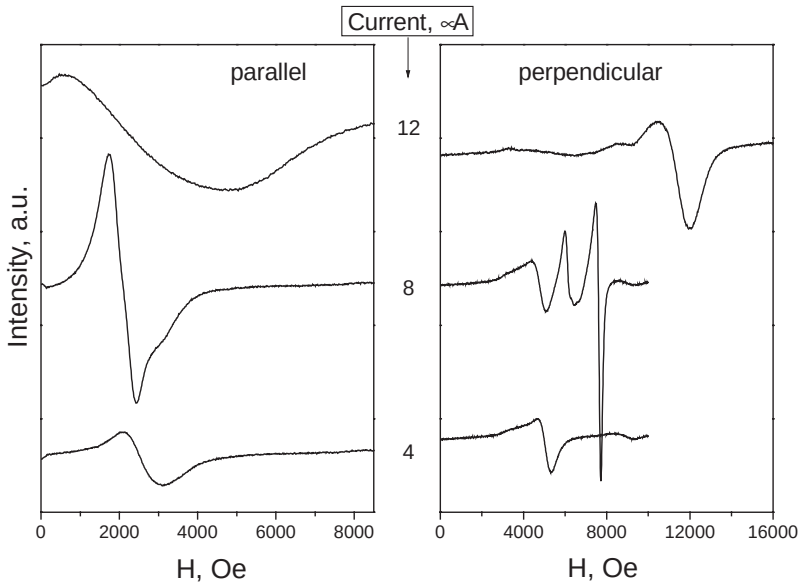

Fig. 3. FMR spectra of the samples implanted with dose of 1.25×10^{17} ions/cm^2 at different ion current densities and subsequently annealed in vacuum. The spectra, measured at parallel and perpendicular orientation of film plane to the magnetic field, are presented at left and right panels, respectively.

for the samples with different implantation doses and varied current densities are presented in Figs. 4a and b, respectively. The g-value for all studied cobalt-implanted PI samples ranges from 2.00 to 2.17 that is close to the g-values found for continuous cobalt films.

Obviously, the granular metal layer in the as-prepared samples consists of small cobalt clusters and particles which are in a superparamagnetic state [14,15] at room temperature. Orientation of the magnetic moments of the particles is affected by thermal fluctuations. Therefore, the magnetic resonance signal cannot be registered if the typical frequency of the fluctuations is appreciably higher than the characteristic frequency of the measuring device, in our case, higher than the microwave frequency which is about 10^{10} Hz. In this situation the signal of magnetic resonance can be observed only when the frequency of the fluctuations decreases below the magnetic resonance frequency, i.e. at low temperatures. In fact, we observe that the FMR signal appears with cooling down to 100 K in the as-prepared samples implanted with doses of 1.25×10^{17} and 1.50×10^{17} ions/cm^2 at an ion current density of $4\,\mu$A/cm^2. On the other hand, the TEM studies indicate that the annealing of the samples increases the particle sizes and results in coagulation and coalescence of the cobalt granules. Therefore, due to the thermal

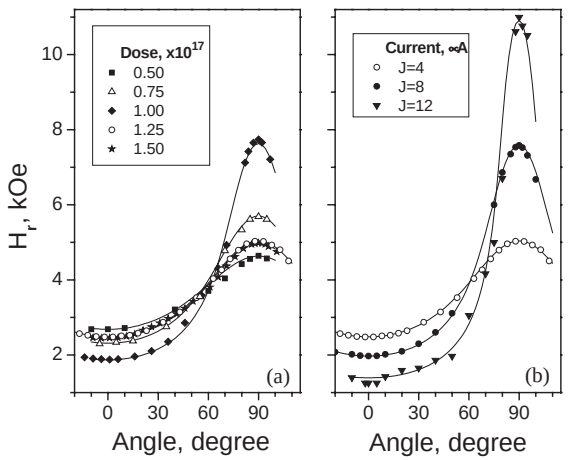

Fig. 4. Dependences of the resonance field on sample orientation in the magnetic field for PI foils implanted with different doses at ion current density of $4\,\mu$A/cm^2 (a) and with the same dose of 1.25×10^{17} ions/cm^2 at different ion current densities (b). The symbols present the experimental values, the lines show the best fits using Eqs. (1) and (2).

treatment at least some part of the cobalt granules form "magnetic" agglomerates with interparticle distances essentially smaller than the particle sizes. The magnetic moments of these agglomerated particles are strongly magnetically coupled to each other either by exchange forces (if there is a direct contact between them) or by dipolar forces and Ruderman–Kittel–Kasuya–Yosida (RKKY) type of interactions via conduction electrons [16] (if the particles do not touch each other).

The RKKY-type mechanism, which depends on the conductivity of the intergranular polymer media, can contribute significantly due to the carbonisation of the irradiated polymer layer [17]. Thus, the "effective magnetic" size of such agglomerates exceeds a critical (so-called "blocking") size beyond which orientations of the magnetic moments are nearly static compared to the magnetoresonance measurement time. As a result, the FMR signal appears in the annealed films. Hence, we can consider the particle agglomeration (increasing the "effective magnetic" size) as a major factor determining the FMR in the cobalt-implanted PI.

It is seen in Figs. 2 and 4a that at low-dose implantation (0.50×10^{17} ions/cm^2) there is only slight anisotropy of the resonance field, while at higher irradiation doses ($\geqslant0.75\times10^{17}$ ions/cm^2) the anisotropy increases significantly. The strong orientational dependence of the FMR signal for high doses is caused by an effect of macroscopic demagnetisation fields in the granular layer. When the distance between the magnetic particles (or particle agglomerates) becomes comparable with their sizes, the dipole–dipole interaction couples the particle magnetic moments. As a result, the granular phase behaves as a united ferromagnetic continuum with respect to dipolar forces even without direct contact between the particles [18]. Hence, the FMR signal originates from the collective motion of the particle magnetic moments, i.e. from the macroscopic magnetisation of the granular layer as a whole system. According to the approach developed in Refs. [18–20], we may interpret the obtained data for the doses from 0.5×10^{17} to 1.50×10^{17} ions/cm^2 as those coming from a thin magnetic film with some effective value of magnetisation and g-factor. Therefore, the resonance condition for the granular film at arbitrary orientation takes the same form as that for a continuous film [21]:

$$\left(\frac{h\nu}{g\beta}\right)^2=(H_r\cos\theta_H-4\pi M_{\rm eff}\cos\theta)^2+H_r\sin\theta_H(H_r\sin\theta_H+4\pi M_{\rm eff}\sin\theta), \quad (1)$$

where ν is resonance frequency, H_r is the magnetic resonance field value, g is the g-factor, $M_{\rm eff}$ is the effective magnetisation, θ and θ_H are out-of-plane angles of magnetisation and DC magnetic field measured from the film normal, respectively. The out-of-plane angle θ is related to θ_H by the equilibrium condition:

$$H_r\sin(\theta-\theta_H)=2\pi M_{\rm eff}\sin2\theta. \quad (2)$$

Eqs. (1) and (2) can be reduced to well known Kittel expressions [22] when $\theta_H=0^\circ$ (magnetic field perpendicular to the plane), and $\theta_H=90^\circ$ (magnetic field parallel to the plane):

$$h\nu=g\beta\cdot(H_r-4\pi M_{\rm eff}),\quad \theta_H=0^\circ, \quad (3)$$

$$h\nu=g\beta\cdot\sqrt{H_r\cdot(H_r+4\pi M_{\rm eff})},\quad \theta_H=90^\circ. \quad (4)$$

Eqs. (1) and (2) may be numerically solved with respect to H_r and θ depending on two parameters: $M_{\rm eff}$ and g. Therefore, the best fits to the experimental data (Fig. 4) allow us to obtain the values of the effective magnetisation and g-factor. The plots of $M_{\rm eff}$ as a function of the implantation dose and ion current density are presented in Fig. 5 and discussed below.

It should be noted that values of the effective magnetisation and g-factor extracted from Eqs. (1) and (2) in general contain also a contribution due to the anisotropy of the particles because of shape or crystallinity. For an ensemble of randomly oriented granules this contribution is averaged to zero but this is not the case if there is some preferential orientation. From this point of view it is remarkable that the dependence of the arbitrary intensity (both on the dose and ion current density) correlates well with that for the effective magnetisation (see plots to the right scale in Fig. 5). It is known that the intensity of the FMR signal is proportional to the total magnetisation of the studied media, i.e. to the bulk value of magnetisation of the ferromagnetic phase times

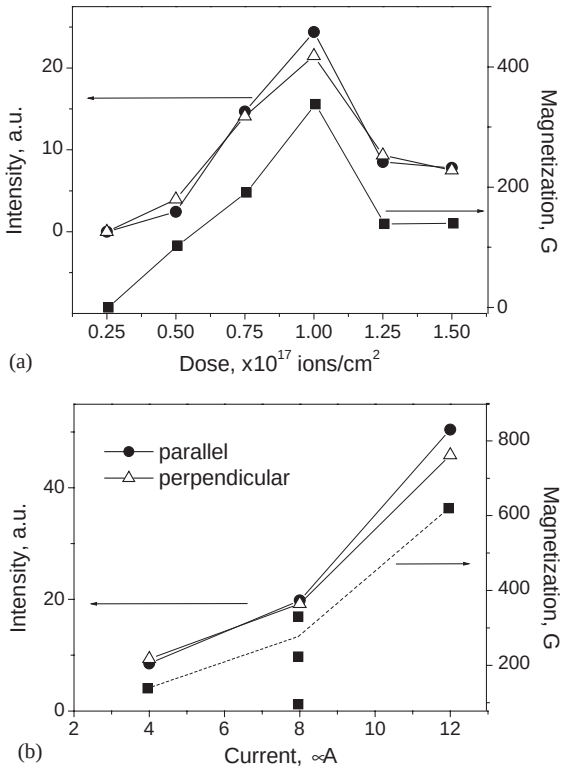

Fig. 5. Dependences of FMR signal intensity and effective magnetisation on the implantation dose (a) and ion current density (b). FMR intensities, extracted from both the parallel and perpendicular orientations, are presented.

the filling factor only, without a contribution due to anisotropic fields. Therefore, this correlation as well as the fact that the extracted effective g-factors in our case are close to the g-value of bulk cobalt justify application of a simple model with nearly spherical particle shapes and the random orientations of the particle crystalline axes. In this model the value of M_{eff} is equal to the volume filling factor, f, times the bulk value of the saturation magnetisation of the ferromagnetic phase ($M_{\text{eff}} = M_S f$). Using the saturation magnetisation value for bulk cobalt ($M_S = 1400$ kOe) we estimated the filling factor of the films (Table 1).

The highest filling factor value of 0.24 corresponds well to the cobalt concentration in the implanted layer, ≈ 25 at%, estimated from the RBS data [13]. One can also see in Fig. 5a the peak in the dose dependences of the intensity and

Table 1
Filling factor (f) versus dose of implantation

Dose ($\times 10^{17}$ ions/cm^2)	0.50	0.75	1.00	1.25	1.50
Filling factor (f)	0.074	0.136	0.241	0.099	0.100

magnetisation near the dose of 1.0×10^{17} ions/cm^2. This shows that the implanted cobalt forms mainly the ferromagnetic phase for the dose of 1.0×10^{17} ions/cm^2.

It has been found [13] that the cobalt atomic concentration increases with the dose, therefore the decrease of the magnetisation (i.e. the filling factor) at high dose is not related to the cobalt content but reflects a decrease in the fraction of the ferromagnetic phase. This may happen if a large portion of small cobalt clusters, which are superparamagnetic at room temperature, are retained after the annealing procedure. Then, the lowering in temperature would freeze the thermal fluctuations of the superparamagnetic phase leading to the increase in the effective magnetisation as well as in the FMR signal intensity [18]. However, our low temperature measurements show minor changes with temperature of the resonance field position, lineshape and integral intensity of the FMR spectra for the samples implanted with higher doses. The decrease in the magnetic phase ratio could also be a result of formation of the non-magnetic cobalt-based compound which is stable under the heating treatment up to 300°C. It is known that with the increase of implantation dose the polymer surface layer undergoes progressive radiation-induced degradation. This results in the carbonisation of the irradiated polymer layer and elimination of volatile components via the latent ion tracks, as was shown in Refs. [13,17]. The XPS studies [17] indicated that in addition to the primary metal cobalt phase some secondary phase, probably a cobalt-oxide or cobalt-carbonyl compound, formed in the layer nearest to the polymer surface (with thickness of about 8 nm). However, the RBS measurements [17,23] showed a strong oxygen depletion up to 10 times compared to the initial value (17.2 at%) in the pristine PI. For instance, in the case of divalent cobalt oxide its fraction will not exceed 25% relative to the metallic cobalt phase, while nearly 100% ratio of

cobalt oxide is needed to explain the observed decrease in filling factor at dose of 1.25×10^{17} ions/cm^2 (Table 1). In contrast, the arbitrary carbon content is strongly increased due to the carbonisation process, forming a layer of amorphous carbon or graphite-like material [17]. Therefore, it is probable that some part of cobalt in the samples implanted with high doses is bonded to the carbon. Formation of Co_3C and Co_2C carbide phases has been reported in the literature before, for example, by 50-keV carbon implantation in cobalt thin films at room temperature [24], and for cobalt–carbon composite thin films prepared by sputter deposition [25]. Thus, we can consider the formation of an additional non-magnetic cobalt-rich phase as the main reason for the decreasing magnetisation of the samples implanted at higher doses.

The filling factor also increases with ion current density as can be observed in both the dependences for effective magnetisation and intensity of the FMR signal (Fig. 5b). It was shown in Ref. [13] that the depth profiles of Co atoms implanted into PI at different ion current densities had similar shape. Nevertheless, our results point out that the magnetic properties of the granular layers formed under the implantation at various current densities are essentially different. We can suggest that at higher ion current densities the concentration of mobile atoms per unit volume of implanted layer increases, thereby stimulating the processes of coagulation and growth of the metallic cobalt particles. As a result, the microstructure and morphology of the synthesised granular metal layers are dissimilar at various ion current densities as well as the lineshapes of the FMR signals (Fig. 3). High ion current densities also cause heating of the sample surface layer due to high local temperatures along the ion tracks. Hence, high ion current densities are equivalent to some extent to annealing. This agrees with the fact that the FMR signal is observed at ion current densities of 8 and 12 μA/cm^2 even in the non-annealed samples. However, there is a significant difference in the time of treatment: the heating due to the high ion current density happens during the implantation process. Obviously, due to this reason the growth and coagulation of the cobalt particles occur at more favourable conditions that prevents the formation of a secondary cobalt-rich phase in the carbonised polymer layer.

In conclusion, Co^+ ions were implanted into PI with an energy of 40 keV and doses in the range of $(0.25–1.50) \times 10^{17}$ ions/cm^2 at ion current densities of 4, 8 and 12 μA/cm^2 at room temperature. TEM investigations showed that the cobalt implantation results in the formation of metal particles with lateral sizes ranging from 5 to 20 nm and they form a granular metal layer with thickness of about 70 nm under the sample surface. The influence of implantation dose, ion current density and post-implantation furnace annealing on the magnetic properties of the synthesised metal–polymer composite layers was studied by the ferromagnetic resonance (FMR) technique. A significant effect of the annealing treatment as well as the high ion current densities on the formation of the ferromagnetic phase in the synthesised composites was found. The effective magnetisation and the metal filling factor for the cobalt granular layers were estimated from the FMR results.

Acknowledgements

This research was supported by the grant No. 02-A-01-02-03 of Research Fund of Gebze Institute of Technology, Turkey, and in part by "Russian Federal Programme for support of leading scientific schools", grant No. SS 1904.2003.2. R.I.K. acknowledges support by the TUBITAK-NATO PC Advanced Fellowship Programme. V.N.P. is grateful to The Swedish Research Council.

References

[1] J.L. Dormann, D. Fiorani (Eds.), Magnetic Properties of Fine Particles, North-Holland, Amsterdam, 1992.
[2] C.J. McHargue, S.X. Ren, J.D. Hunn, Mater. Sci. Eng. A 253 (1998) 1.
[3] E.M. Hunt, J.M. Hampikian, Acta Mater. 5 (1999) 1497.
[4] A. Meldrum, L.A. Boatner, C.W. White, Nucl. Instrum. Methods B 178 (2001) 7.
[5] R. White, Data Storage 4 (1997) 55.
[6] H. Brückl, G. Reiss, H. Vinzelberg, M. Bertram, I. Mönch, J. Schumann, Phys. Rev. B 58 (1998) 8893.

[7] N.C. Koon, D. Weber, P. Pehrsson, A.I. Shindler, Mater. Res. Soc. Symp. Proc. 27 (1984) 445.
[8] K. Ogava, United State Patent, No. 4.751.100, 1988.
[9] V. Petukhov, V. Zhikharev, M. Ibragimova, E. Zheglov, V. Bazarov, I. Khaibullin, Solid State Commun. 97 (1996) 361.
[10] I.B. Khaibullin, R.I. Khaibullin, S.N. Abdullin, A.L. Stepanov, Yu.N. Osin, V.V. Bazarov, S.P. Kurzin, Nucl. Instrum. Methods B 127–128 (1997) 685.
[11] R.I. Khaibullin, V.A. Zhikharev, Yu.N. Osin, E.P. Zheglov, I.B. Khaibullin, B.Z. Rameev, B. Aktas, Nucl. Instr. and Methods B 166–167 (2000) 897.
[12] R.I. Khaibullin, V.N. Popok, V.V. Bazarov, E.P. Zheglov, B.Z. Rameev, C. Okay, L.R. Tagirov, B. Aktas, Nucl. Instrum. Methods B 191 (2002) 810.
[13] V.N. Popok, R.I. Khaibullin, V.V. Bazarov, V.F. Valeev, V. Hnatowicz, A. Mackova, V.B. Odzhaev, Nucl. Instrum. Methods B. 191 (2002) 695.
[14] C.P. Bean, J. Appl. Phys. 26 (1955) 1381.
[15] L. Néel, Ann. Geophys. 5 (1949) 99.
[16] Yu.G. Pogorelov, G.N. Kakazei, M.M.P. de Azevedo, J.B. Sousa, J. Magn. Magn. Mater. 196–197 (1999) 112.
[17] V.N. Popok, R.I. Khaibullin, A. Toth, V. Beshliu, V. Hnatowicz, A. Mackova, Surf. Sci. 532–535 (2003) 1034.
[18] G.N. Kakazei, A.F. Kravets, N.A. Lesnik, M.M. Pereira de Azevedo, Yu.G. Pogorelov, J.B. Sousa, Appl. Phys. 85 (1999) 5654.
[19] U. Netzelmann, J. Appl. Phys. 68 (1990) 1800.
[20] J. Dubowik, Phys. Rev. B 54 (1996) 1088.
[21] A. Butera, J.N. Zhou, J.A. Barnard, Phys. Res. B 60 (1999) 12270.
[22] C. Kittel, Introduction to Solid State Physics, 7th Edition, Wiley, New York, USA, 1996, p. 505.
[23] A. Mackova, V. Hnatowicz, V. Peřina, V.N. Popok, R.I. Khaibullin, V.V. Bazarov, V.B. Odzhaev, Surf. Coat. Technol. 158–159 (2002) 395.
[24] B.X. Liu, J. Wang, Z.Z. Fang, J. Appl. Phys. 69 (1991) 7342.
[25] J.-J. Delaunay, T. Hayashi, M. Tomita, S. Hirono, J. Appl. Phys. 82 (1997) 2200.